# Redox-based resistive switching in ferroelectric perovskite nanotubes

Stephen S. Nonnenmann, Eric M. Gallo, and Jonathan E. Spanier[a)]
*Department of Materials Science and Engineering, Drexel University, Philadelphia, Pennsylvania 19104, USA*

(Received 24 June 2010; accepted 12 August 2010; published online 10 September 2010)

Hysteresis in current and ferroelectric piezoelectric phase were collected across the walls of individual, electrically interfaced lead zirconate titanate (PZT) nanotubes. The nanotubes exhibit average on/off current ratios of ~10 and ~1000 in static local probe and top-electroded configurations, respectively. Reversibility in conduction state of an individual nanotube following different stages of an $O_2$-rich/$O_2$-deficient/$O_2$-rich anneal cycle provide evidence of an oxygen vacancy concentration-based conduction mechanism. © *2010 American Institute of Physics*. [doi:10.1063/1.3486224]

Recent developments in the synthesis of ferroelectric (FE) nanostructures, e.g., monodisperse nanoparticles[1] and nanocubes,[2] nanowires,[3,4] and nanotubes,[5,6] and the effects of finite curvature[7,8] have renewed interest in the miniaturization of FE systems for use as next generation memory elements. Thin-film FE materials have also attracted interest as current-based switching elements due to their large resistance ratios and nondestructive readout states.[9,10] Resistive switching has been observed in a number of thin-film and nanostructured oxide materials, including in thin-film binary oxides $TiO_2$,[11,12] $ZrO_2$,[13] and $MnO_2$,[14] in binary oxide (NiO) heterostructure-based nanowires,[15] and in other thin-film $ABO_3$ oxide perovskites,[16–19] adding greater functionality to known FE properties in developing memory applications.

Observed resistive behavior in FE materials has been explained in terms of either tunneling or defect-mediated mechanisms. In recent work a charge trap conduction model has been proposed, whereby charges are injected via Fowler–Nordheim tunneling[9] and trapped within defects, a mechanism strongly dependent upon polarization orientation, particularly at the metal/FE interface.[20–23] Others have proposed a filamentary conduction mechanism[24] via electroformation and electromigration of extended defects such as oxygen vacancies[25,26] and dislocations[19,27] within materials possessing mixed valence character, thus attributing conduction to anion transport. To date, studies of resistive switching in FE oxides have involved exclusively thin films. In this paper we report on the resistive switching within individual FE oxide perovskite nanotubes possessing noble-metal (Au) nanowire cores. We observe the resistive and FE switching in these nanostructures, and we provide experimental evidence for an oxygen vacancy concentration-mediated electroresistance.

Details of the synthesis method and structural characterizations of, and electrical contacting methods for Au-filled $Pb(Zr_{0.52}Ti_{0.48})O_3$ (PZT) nanotubes employed for this study have been presented elsewhere.[28] The local probe setup allowing simultaneous collection of FE piezoelectric phase hysteresis and resistive current-voltage response of an individual Au-PZT core-shell nanowire (50 nm diameter, 7 nm shell thickness) is depicted in Fig. 1(a). Here a cantilever holder containing a built-in transimpedance amplifier (ORCA™, Asylum Research) was used to measure the FE and resistive switching simultaneously.[18,22] An electrically grounded cantilever tip (Olympus AC240TM) was placed in contact with the PZT nanotube surface [Fig. 1(b)], employing constant-deflection feedback. In a typical experiment a waveform consisting of a low-frequency zero-offset triangular component (3 Hz, $\pm 16$ $V_{pp}$) and a higher frequency component (10 kHz, 2 $V_{ac}$) was applied to the nanowire core (inner electrode) during a deflection-triggered force-pull sequence in which the cantilever was in continuous contact and constant deflection feedback, thus allowing collection of the FE piezoelectric deflection phase signal [Fig. 1(c); left axis] and resistive current [Fig. 1(c); right axis] through the nanotube wall.

The FE phase signal exhibits a distinct offset along the voltage axis [Fig. 1(c)]. This offset can be attributed to an electrostatic potential gradient arising from the finite curvature of the shell,[8] from different surface chemical environments of the inner and outer surfaces of the nanotube, and differences in metal work function between the inner electrode (Au) and the cantilever tip coating (Pt). Observed vertical shifts indicate a preferred polarization orientation,[22] previously shown for FE nanoshells as a result of curvature-driven polarization gradients.[8] The observed electroresistance in the nanotube wall [Fig. 1(c), right axis] can be described by an equivalent circuit consisting of a diode set in parallel with a single resistor that is split by a switch.[12] In a voltage sweep cycle (from 0 V) the resulting resistive switching character is highly blocking (diode-like) in the first quarter, then substantially less blocking (nearly Ohmic) during the second and third quarters, then it returns to highly blocking in the final quarter, as seen in the collected I-V trace [Fig. 1(c)].

Notably, the observed width of the electroresistive switching voltage hysteresis $|V_{cr+}-V_{cr-}|$ is comparable to that for the FE coercive voltage $V_C$, aside from a voltage offset. The on/off current ratios approach $10^3$, with a measured on-current value of 20 nA. This current value, however, is orders of magnitude lower than those for typical resistive memory elements ($\mu$A-mA).[25] The observed reduction in the scale of currents reported implies a current limit exists and may be due to Fowler–Nordheim tunneling between the probe tip and nanotube surface, similar to current response shown in FE thin films.[9] This is not surprising given the scale of the atomic force microscopy (AFM) probe

a)Electronic mail: spanier@drexel.edu.

 

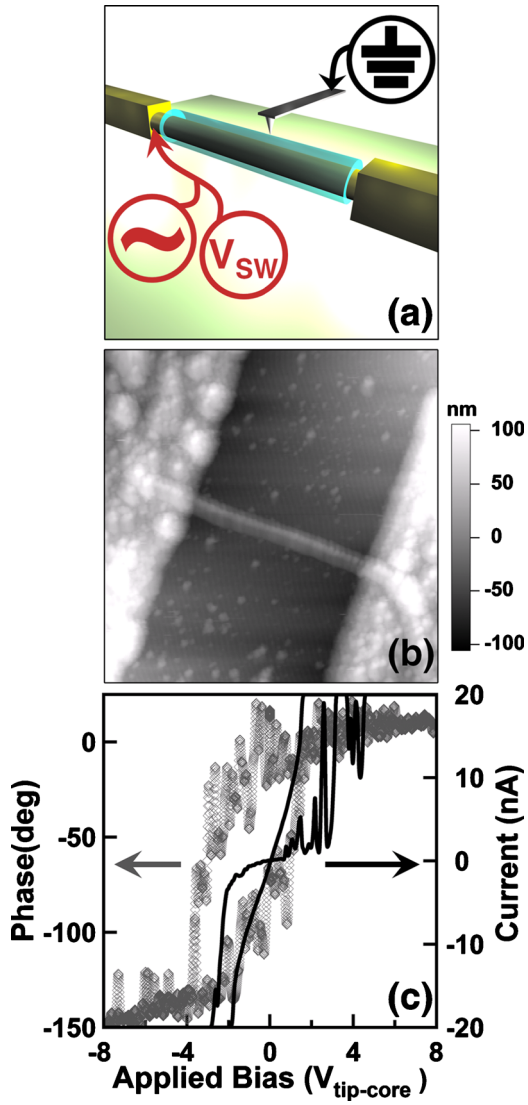


FIG. 1. (Color online) (a) Schematic of IV-hysteresis collection where an arbitrary waveform consisting of two frequency components is applied directly to the Au-core inner electrode, as described in the main text. (b) Topographic AFM height image of a contacted 50 nm core-shell nanostructure (scan size $5\times5$ $\mu m^2$). (c) FE piezoelectric hysteresis (gray markers, left axis) and resistive current-voltage (black line, right axis) collected simultaneously. The bias $V_{core\text{-}tip}$ is applied to nanowire core.

tip (~30 nm diameter) in relation to the size of electrical contacts used in other electroresistance switching experiments involving thin films.[18]

These nanostructures may be considered as candidate electroresistive and FE memory elements in which each nanowire contains one or more distinct switching elements within the shell portion of these core-shell nanowires using fixed electrodes. Electrical contacts to the Au nanowire cores [Fig. 2(a); false color: blue] were made using electron beam lithography, wet etching, and resistive thermal evaporation (10 nm Cr and 150 nm Au). Electron beam-induced deposition of Pt using a dual-beam FIB-SEM (FEI DB235) was carried out, producing a $500\times100$ $nm^2$ electrode of 250 nm in height on the outer surface of the nanowire [Fig. 2(a); false color: red]. Current-voltage traces were collected in vacuum through the nanotube wall between the top electrode (shell) and left nanowire-core electrode (core). Shown in Fig. 2(b) is the collected resistive current-voltage response of a segment of the core-shell test structure; the measured current values are denoted by the sequence (i)–(vi). The observed on-current value greatly increased (30 $\mu$A) with respect to the proximal probe measurements (20 nA). The average on/off current ratios in the shell-electrode nanostructures were typically ~10 [Fig. 2(c)].

To ascertain the underlying mechanism driving the observed electroresistances, the fixed electroded test structures were subjected to an annealing cycle consisting of $O_2$-rich/$O_2$-deficient/$O_2$-rich steps, with collection of the I-V response following each step. Following collection of the initial I-V response of the as-prepared shell-electroded test structures [Fig. 2(b)], the structures were annealed for 1 h at 450 °C under a constant flow of 100 SCCM (SCCM denotes cubic centimeter per minute at STP)$O_2$ (Airgas UHP) at a base pressure of 2 Torr ("$O_2$-rich"). After the first $O_2$-rich step the I-V character of the shell-electroded test structures was seen to exhibit a ~$10^3$-fold decrease in current [Fig. 3(a)]. The nanostructures were then subjected to a forming gas anneal for 1 h at 450 °C under a constant flow of 100 SCCM 95%$N_2$-5%$H_2$ (Airgas HINY200) at a base pressure of 2 Torr ("$O_2$-deficient"). The collected $O_2$-deficient I-V response [Fig. 3(b)] possessed a ~$10^5$ increase in current ($I>150$ $\mu$A) manifested by the onset of resistive switching, with a on/off ratio of ~$10^4$. A final $O_2$-rich anneal step (450 °C, 5 h, 2 Torr) was performed to confirm the reversibility of the oxygen mechanism for conduction within the PZT nanoshell [Fig. 3(c)]. The increased anneal time was selected to promote the filling of the $O_2$ vacancies created during the $O_2$-deficient anneal with oxygen atoms.

These results indicate an oxygen defect concentration-mediated conduction process. The higher conduction state observed in Fig. 3(b) is attributed to formation of oxygen vacancies in an $O_2$-deficient or low $p_{O_2}$ environment. From

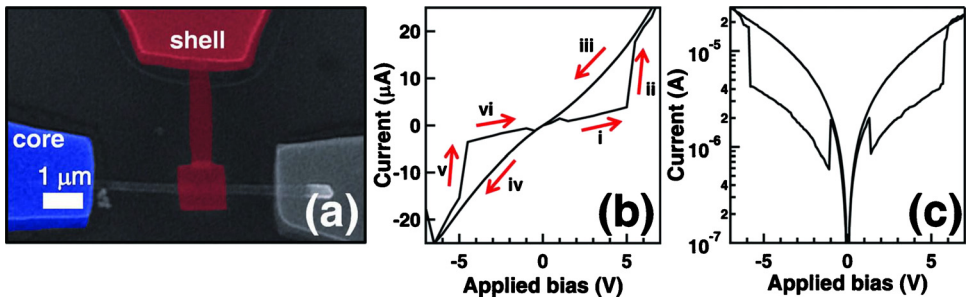


FIG. 2. (Color online) (a) SEM image of top-electroded core-shell nanostructure, showing measurement path between Pt-top electrode (red, labeled shell) and left nanowire-core electrode (blue, labeled core) (scalebar=1 $\mu$m). (b) Representative resistive current-voltage character of a shell-electroded Au-core, PZT-shell nanostructure. (c) Log-based plot of current-voltage showing an order of magnitude difference in current across the finite-thickness direction of the core-shell nanostructure.

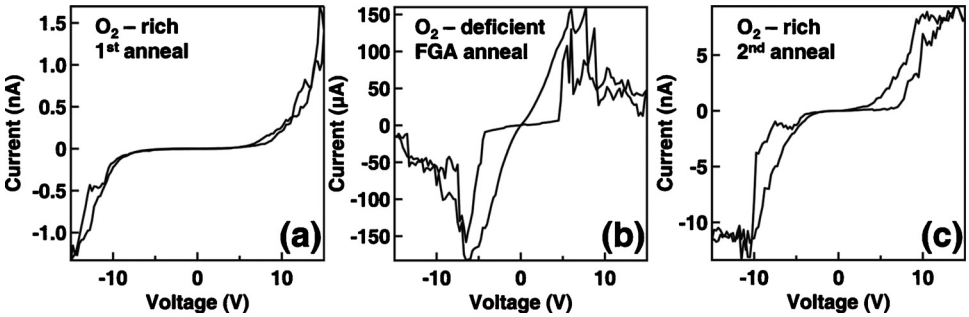


FIG. 3. Current-voltage sweeps of a Au-PZT core-shell nanowires after an (a) $O_2$-rich, (b) $O_2$-deficient, and (c) $O_2$-rich annealing cycle.

the general form for a nonstoichiometric perovskite, the defect reaction for a B-site rich titanate, such as PZT, becomes[29]

$$TiO_2 \xrightarrow{Pb(Zr,Ti)O_3} Ti_{Ti}^{X} + 2O_O^{X} + V''_{Pb} + V_O^{**},$$

where oxygen vacancies assist the conduction process by yielding electrons, as follows:

$$O_O^{X} \rightarrow V_O^{**} + \tfrac{1}{2}O_{2(g)} + 2e'.$$

Considering the strong dependence of oxygen vacancy concentration on oxygen partial pressure, we propose that the large differences observed in current between the $O_2$-rich and $O_2$-deficient anneal steps may be explained through vacancy formation, as previously shown in $TiO_2$-based nanotubes via electron paramagnetic resonance.[30] The onset of resistive switching after an $O_2$-deficient anneal suggests that a critical oxygen vacancy concentration is necessary for a switching event. The results shown in Fig. 3(b) are also consistent with a filamentary conduction mechanism including, e.g., the proposed formation of transition metal anion nanofilaments along the grain boundaries of polycrystalline grains[24,31] due to oxygen migration.

We have demonstrated collection of FE switching and electroresistance in an individual PZT nanoshell across the finite, shell-normal direction, and the electroresistance switching within a segment of the nanoshell possessing a fixed electrode. The large on/off current ratios $(10^1-10^4)$ are consistent with an oxygen vacancy-mediated transport mechanism. Nanostructures subjected to controlled oxygen environments consisting of a $O_2$-rich/$O_2$-deficient/$O_2$-rich anneal cycle exhibited $O_2$-deficient/$O_2$-rich current ratios of $\sim 10^5$. This model system and results presented demonstrate further the potential of electrically interfaced $ABO_3$ FE oxide perovskite nanoshells for use as nonvolatile memories and as oxygen sensing elements via FE and electroresistive switching. We believe demonstration of electroresistive and FE switching along the finite dimension within these nanotubes as shown here will encourage further interest in investigating and exploiting the properties of high functional density oxide nanostructures.

We thank Michael Coster, Guannan Chen, Terrence McGuckin, and Jason Bemis for assistance with sample preparation, nanofabrication, and interfacing. This work was supported by the Materials Sciences Division of the Army Research Office (Grant No. W911NF-08-1-0067). We also acknowledge support for instrumentation from the NSF (Grant No. DMR-0722845).

[1]S. O'Brien, L. Brus, and C. B. Murray, J. Am. Chem. Soc. **123**, 12085 (2001).
[2]S. Adireddy, C. Lin, B. Cao, W. Zhou, and G. Caruntu, Chem. Mater. **22**, 1946 (2010).
[3]J. Spanier, A. Kolpak, J. Urban, I. Grinberg, L. Ouyang, W. Yun, A. Rappe, and H. Park, Nano Lett. **6**, 735 (2006).
[4]X. Y. Zhang, X. Zhao, C. W. Lai, J. Wang, and J. Y. Dai, Appl. Phys. Lett. **85**, 4190 (2004).
[5]B. A. Hernandez, K.-S. Chang, E. R. Fisher, and P. K. Dorhout, Chem. Mater. **14**, 480 (2002).
[6]Y. Luo, I. Szafraniak, N. D. Zakharov, V. Nagarajan, M. Steinhart, R. B. Wehrspohn, J. H. Wendorff, R. Ramesh, and M. Alexe, Appl. Phys. Lett. **83**, 440 (2003).
[7]A. N. Morozovska, E. A. Eliseev, and M. D. Glinchuk, Phys. Rev. B **73**, 214106 (2006).
[8]S. S. Nonnenmann, O. D. Leaffer, E. M. Gallo, M. T. Coster, and J. E. Spanier, Nano Lett. **10**, 542 (2010).
[9]P. Maksymovych, S. Jesse, P. Yu, R. Ramesh, A. P. Baddorf, and S. V. Kalinin, Science **324**, 1421 (2009).
[10]V. Garcia, S. Fusil, K. Bouzehouane, S. Enouz-Vedrenne, N. D. Mathur, A. Barthelemy, and M. Bibes, Nature (London) **460**, 81 (2009).
[11]Y. Watanabe and M. Okano, J. Appl. Phys. **94**, 7187 (2003).
[12]J. J. Yang, M. D. Pickett, X. Li, D. A. A. Ohlberg, D. R. Stewart, and R. S. Williams, Nat. Nanotechnol. **3**, 429 (2008).
[13]A. Beck, J. G. Bednorz, Ch. Gerber, C. Rossel, and D. Widmer, Appl. Phys. Lett. **77**, 139 (2000).
[14]A. Sawa, T. Fujii, M. Kawasaki, and Y. Tokura, Appl. Phys. Lett. **85**, 4073 (2004).
[15]K. Oka, T. Yanagida, K. Nagashima, H. Tanaka, and T. Kawai, J. Am. Chem. Soc. **131**, 3434 (2009).
[16]J. Rodrı´guez Contreras, H. Kohlstedt, U. Poppe, R. Waser, C. Buchal, and N. A. Pertsev, Appl. Phys. Lett. **83**, 4595 (2003).
[17]R. Oligschlaeger, R. Waser, R. Meyer, S. Karthaeuser, and R. Dittmann, Appl. Phys. Lett. **88**, 042901 (2006).
[18]H. Kohlstedt, A. Petraru, K. Szot, A. Rüdiger, P. Mueffels, H. Haselier, R. Waser, and V. Nagarajan, Appl. Phys. Lett. **92**, 062907 (2008).
[19]K. Szot, W. Speier, G. Bihlmayer, and R. Waser, Nature Mater. **5**, 312 (2006).
[20]H. Kohlstedt, N. A. Pertsev, J. Rodríguez Contreras, and R. Waser, Phys. Rev. B **72**, 125341 (2005).
[21]M. Y. Zhuravlev, R. F. Sabirianov, S. S. Jaswal, and E. Y. Tsymbal, Phys. Rev. Lett. **94**, 246802 (2005).
[22]A. Gruverman, D. Wu, H. Lu, Y. Wang, H. W. Jang, C. M. Folkman, M. Ye. Zhuravlev, D. Felker, M. Rzchowski, C. B. Eom, and E. Y. Tsymbal, Nano Lett. **9**, 3539 (2009).
[23]P. W. M. Blom, R. M. Wolf, J. F. M. Cillessen, and M. P. C. M. Krijn, Phys. Rev. Lett. **73**, 2107 (1994).
[24]M.-J. Lee, S. Han, S. H. Jeon, B. H. Park, B. S. Kang, S.-E. Ahn, K. H. Kim, C. B. Lee, C. J. Kim, I.-K. Yoo, D. H. Seo, X.-S. Li, J.-B. Park, J.-H. Lee, and Y. Park, Nano Lett. **9**, 1476 (2009).
[25]R. Waser, R. Dittmann, G. Staikov, and K. Szot, Adv. Mater. **21**, 2632 (2009).
[26]Y. Watanabe, Ferroelectrics **349**, 190 (2007).
[27]R. Waser and M. Aono, Nature Mater. **6**, 833 (2007).
[28]S. S. Nonnenmann, E. G. Gallo, M. T. Coster, G. R. Soja, C. L. Johnson, R. S. Joseph, and J. E. Spanier, Appl. Phys. Lett. **95**, 232903 (2009).
[29]S. Lee, G. A. Rossetti, Z.-K. Liu, and C. A. Randall, J. Appl. Phys. **105**, 093519 (2009).
[30]J. M. Cho, J. M. Seo, J.-K. Lee, H. Zhang, and R. Lamb, Physica B **404**, 127 (2009).
[31]K. Tsunoda, Y. Fukuzumi, J. R. Jameson, Z. Wang, P. B. Griffin, and Y. Nishi, Appl. Phys. Lett. **90**, 113501 (2007).